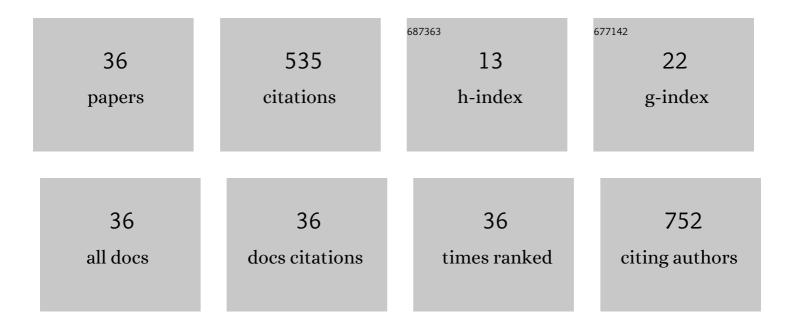
Nicolas Finck

List of Publications by Year in descending order

Source: https://exaly.com/author-pdf/3324749/publications.pdf Version: 2024-02-01



#	Article	IF	CITATIONS
1	Uranium Redox Transformations after U(VI) Coprecipitation with Magnetite Nanoparticles. Environmental Science & Technology, 2017, 51, 2217-2225.	10.0	112
2	Adsorption of Selenium and Strontium on Goethite: EXAFS Study and Surface Complexation Modeling of the Ternary Systems. Environmental Science & amp; Technology, 2017, 51, 3751-3758.	10.0	62
3	Macroscopic and spectroscopic investigations on Eu(III) and Cm(III) sorption onto bayerite (β-Al(OH)3) and corundum (α-Al2O3). Journal of Colloid and Interface Science, 2016, 461, 215-224.	9.4	30
4	Montmorillonite colloids: I. Characterization and stability of dispersions with different size fractions. Applied Clay Science, 2015, 114, 179-189.	5.2	26
5	Sites of Lu(III) Sorbed to and Coprecipitated with Hectorite. Environmental Science & Technology, 2009, 43, 8807-8812.	10.0	22
6	Adsorption of arsenic(V) onto single sheet iron oxide: X-ray absorption fine structure and surface complexation. Journal of Colloid and Interface Science, 2019, 554, 433-443.	9.4	20
7	Selenide Retention by Mackinawite. Environmental Science & amp; Technology, 2012, 46, 10004-10011.	10.0	18
8	Temperature effects on the surface acidity properties of zirconium diphosphate. Journal of Colloid and Interface Science, 2007, 312, 230-236.	9.4	16
9	High level nuclear waste glass corrosion in synthetic clay pore solution and retention of actinides in secondary phases. Journal of Nuclear Materials, 2009, 385, 456-460.	2.7	16
10	Structural iron in dioctahedral and trioctahedral smectites: a polarized XAS study. Physics and Chemistry of Minerals, 2015, 42, 847-859.	0.8	16
11	Am(III) coprecipitation with and adsorption on the smectite hectorite. Chemical Geology, 2015, 409, 12-19.	3.3	15
12	Trivalent Actinide Uptake by Iron (Hydr)oxides. Environmental Science & Technology, 2016, 50, 10428-10436.	10.0	15
13	Tetrahedral charge and Fe content in dioctahedral smectites. Clay Minerals, 2017, 52, 51-65.	0.6	15
14	Temperature effects on the interaction mechanisms between U(VI) and Eu(III) and ZrP ₂ O ₇ : experiment and modelling. Radiochimica Acta, 2008, 96, 11-21.	1.2	12
15	Chemical status of U(VI) in cemented waste forms under saline conditions. Radiochimica Acta, 2010, 98, 674-683.	1.2	11
16	Sorption of americium / europium onto magnetite under saline conditions: Batch experiments, surface complexation modelling and X-ray absorption spectroscopy study. Journal of Colloid and Interface Science, 2020, 561, 708-718.	9.4	11
17	Reactive Transport Modelling of the Long-Term Interaction between Carbon Steel and MX-80 Bentonite at 25 °C. Minerals (Basel, Switzerland), 2021, 11, 1272.	2.0	11
18	TRLFS characterization of Eu(III)-doped synthetic organo-hectorite. Journal of Contaminant Hydrology, 2008, 102, 253-262.	3.3	10

NICOLAS FINCK

#	Article	IF	CITATIONS
19	Interaction of selenite with reduced Fe and/or S species: An XRD and XAS study. Journal of Contaminant Hydrology, 2016, 188, 44-51.	3.3	9
20	Yttrium co-precipitation with smectite: A polarized XAS and AsFIFFF study. Applied Clay Science, 2017, 137, 11-21.	5.2	9
21	Treatment of temperature dependence of interfacial speciation by speciation codes and temperature congruence of oxide surface charge. Applied Geochemistry, 2019, 102, 26-33.	3.0	9
22	Flow field-flow fractionation (FIFFF) coupled to sensitive detection techniques: a way to examine radionuclide interactions with nanoparticles. Mineralogical Magazine, 2012, 76, 2709-2721.	1.4	8
23	Aqueous U(VI) interaction with magnetite nanoparticles in a mixed flow reactor system: HR-XANES study. Journal of Physics: Conference Series, 2016, 712, 012086.	0.4	8
24	Structural iron in smectites with different charge locations. Physics and Chemistry of Minerals, 2019, 46, 639-661.	0.8	8
25	Characterization of Eu(III) co-precipitated with and adsorbed on hectorite: from macroscopic crystallites to nanoparticles. Mineralogical Magazine, 2012, 76, 2723-2740.	1.4	7
26	XAS signatures of Am(III) adsorbed onto magnetite and maghemite. Journal of Physics: Conference Series, 2016, 712, 012085.	0.4	7
27	Adsorption of Strontium onto Synthetic Iron(III) Oxide up to High Ionic Strength Systems. Minerals (Basel, Switzerland), 2021, 11, 1093.	2.0	7
28	Characterization and radionuclide retention properties of heat-treated concrete. Physics and Chemistry of the Earth, 2014, 70-71, 45-52.	2.9	5
29	Fate of Lu(III) sorbed on 2-line ferrihydrite at pHÂ5.7 and aged for 12Âyears at room temperature. I: insights from ICP-OES, XRD, ESEM, AsFIFFF/ICP-MS, and EXAFS spectroscopy. Environmental Science and Pollution Research, 2019, 26, 5238-5250.	5.3	4
30	Fate of Lu(III) sorbed on 2-line ferrihydrite at pHÂ5.7 and aged for 12Âyears at room temperature. II: insights from STEM-EDXS and DFT calculations. Environmental Science and Pollution Research, 2019, 26, 5282-5293.	5.3	4
31	Fluorescence X-ray Absorption Study of ScCl ₃ -Doped Sodium Alanate. Journal of Physical Chemistry C, 2015, 119, 15810-15815.	3.1	3
32	Retention of Iodide and Chloride by Formation of a Green Rust Solid Solution GR-Cl1–xIx: A Multiscale Approach. Inorganic Chemistry, 2021, 60, 10585-10595.	4.0	3
33	Synthetic Smectite Colloids: Characterization of Nanoparticles after Co-Precipitation in the Presence of Lanthanides and Tetravalent Elements (Zr, Th). Chromatography (Basel), 2015, 2, 545-566.	1.2	2
34	First Principle Investigation of the Incorporation of Trivalent Lanthanides and Actinides in Hydroxycarbonate and Hydroxychloride Green Rust. Journal of Physical Chemistry C, 2022, 126, 8016-8028.	3.1	2
35	Iron speciation in Opalinus clay minerals. Applied Clay Science, 2020, 193, 105679.	5.2	1
36	Unexpected behavior of sodium sulfate observed in experimental freezing and corrosion studies. Journal of Raman Spectroscopy, 2021, 52, 1499-1506.	2.5	1